5. Data Interpretation

A. THE NATURE OF THE SPECTRUM

(1) General Features. The spectrum is displayed as a plot of electron binding energy versus the number of electrons in a fixed, small energy interval. The position on the kinetic energy scale equal to the photon energy minus the spectrometer work function corresponds to a binding energy of zero with reference to the Fermi level (equation 1). Therefore, a binding energy scale beginning at that point and increasing to the left is customarily used.

The spectra in this Handbook are typical for the various elements. The well-defined peaks are due to electrons that have not lost energy in emerging from the sample. Electrons that have lost energy form the raised background at binding energies higher than the peaks. The background is continuous because the energy loss processes are random and multiple.

The "noise" in the spectrum is not instrumental, but is the consequence of the collection of single electrons as counts randomly spaced in time. The standard deviation for counts collected in any channel is equal to the square root of the counts, so that the percent standard deviation is $100/(\text{counts})^{1/2}$. The signal/noise ratio is then proportional to the square root of the counting time. The background level upon which the peak is superimposed is a characteristic of the specimen and the transmission characteristics of the instrument.

(2) Kinds of Lines. Several types of peaks are observed in ESCA spectra. Some are fundamental to the technique, and are always observed. Others are dependent upon the exact physical and chemical nature of the sample. The following describes the various spectral features that are likely to be encountered.

i. Photoelectron Lines. The most intense of the photoelectron lines are usually relatively symmetrical and are typically the narrowest lines observed in the spectrum. Photoelectron lines of pure metals can, however, exhibit considerable asymmetry due to coupling with conduction electrons. Peak width is a convolution of the natural line width, the width of the x-ray line and the instrumental contribution to the line width. Less intense photoelectron lines at higher binding energies are usually wider by 1-4 eV than the lines at lower binding energies. All of the photoelectron lines of insulating solids are of the order of 0.5 eV wider than photoelectron lines of conductors. The approximate binding energies of all photoelectron lines detectable are catalogued in Tables 1-4 of the Appendix.

ii. Auger Lines. These are, more properly, groups of lines in rather complex patterns. There are four main Auger series observable in ESCA. They are the KLL, LMM, MNN, and NOO series, identified by specifying the initial and final vacancies in the Auger transition. The KLL series, for example, includes those processes with an initial vacancy in the K shell and final double vacancy in the L shell. The symbol V, e.g. KVV, indicates that the final vacancies are in valence levels. The KLL series has, theoretically, nine lines and others have

still more. Since Auger lines have kinetic energies that are independent of the ionizing radiation they appear on a binding energy plot to be in different positions when ionizing photons of different energy (i.e. different x-ray sources) are used. Core-type Auger lines (with final vacancies deeper than the valence levels) usually have at least one component of intensity and width similar to the most intense photoelectron line. Positions of the more prominent Auger components are catalogued along with the photoelectron peaks in Tables 1 through 4 in the Appendix.

iii. X-ray Satellites. The x-ray emission spectrum used for irradiation exhibits not only the characteristic x-ray, but some minor x-ray components at higher photon energies. For each photoelectron peak that results from the Kα x-ray photons, there is a family of minor peaks at lower binding energies, with intensity and spacing characteristic of the x-ray anode material. The pattern of such satellites for Mg and Al is shown in Figure 6 and Table 1.

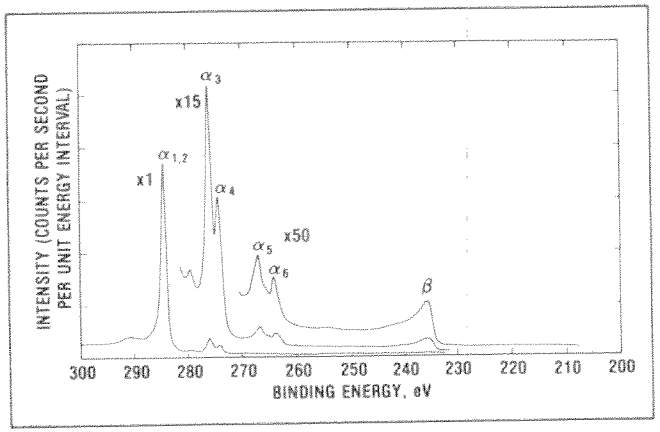

Figure 6. Mg x-ray satellites (C1s graphite spectrum).

Table 1 — X-ray satellite energies and intensities

		$\alpha_{1,2}$	α_3	α_4	α_5	α_6	β
Mg	displacement, eV	0	8.4	10.2	17.5	20.0	48.5
	relative height	100	8.0	4.1	0.55	0.45	0.5
Al	displacement, eV	0	9.8	11.8	20.1	23.4	69.7
	relative height	100	6.4	3.2	0.4	0.3	0.55

iv. X-ray "Ghosts". Occasionally x-radiation from an element other than the x-ray source anode material impinges upon the sample, resulting in small peaks corresponding to the most intense spectral peaks, but displaced by a characteristic energy interval. These lines can be due to Mg impurity in the Al anode, or vice versa, Cu from the anode base structure or generation of x-ray photons in the aluminum foil x-ray window. On occasion, such lines can originate via generation of x-rays within the sample itself. This last possibility is rare, because the probability of x-ray emission is low relative to the Auger transition. Nevertheless, such minor lines can be puzzling. Table 2 indicates where such peaks are most likely to occur, relative to the most intense photoelectron lines. Since the appearance of "ghost" lines is a rare occurrence, they should not be considered in line identification until all other possibilities are excluded.

Table 2 — Displacements of x-ray "ghost" lines

(Apparent binding energy of the "ghost" line minus that of the parent photoelectron line.)

Contaminating Radiation	Anode Material	
	Mg	Al
O (Kα)	728.7	961.7
Cu (Lα)	323.9	556.9
Mg (Kα)	—	233.0
Al (Kα)	-233.0	—

v. Shake-Up Lines. Not all photoelectric processes are simple ones, leading to the formation of ions in the ground state. Rather often, there is a finite probability that the ion will be left in an excited state, a few electron volts above the ground state. In this event, the kinetic energy of the emitted photoelectron is reduced, with the difference corresponding to the energy difference between the ground state and the excited state. This results in the formation of a satellite peak a few electron volts lower in kinetic energy (higher in binding energy) than the main peak. As an example, the characteristic shake-up line for carbon in unsaturated compounds, a shake-up process involving the energy of the $\pi \rightarrow \pi^*$ transition, is shown in Figure 7.

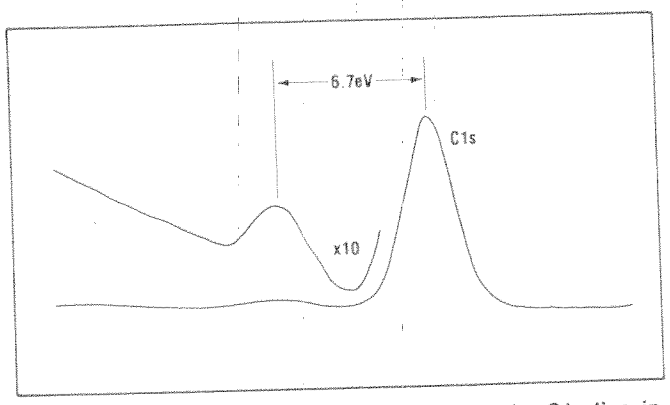

Figure 7. **The π-bond shake-up satellite for the C1s line in polystyrene.**

In some cases, most often with paramagnetic compounds, the intensity of the shake-up satellite may approach that of the main line. More than one satellite of a principal photoelectron line can also be observed, as shown in Figure 8. The occurrence of such lines is sometimes more apparent in Auger spectral contours, of which

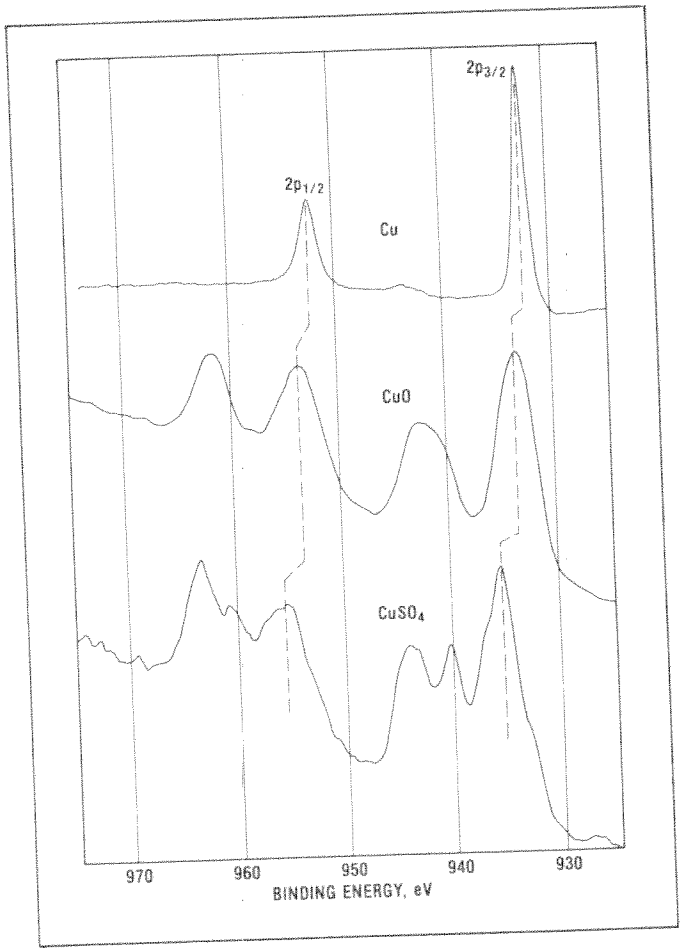

Figure 8. **Examples of shake-up lines observed with the copper 2p spectrum.**

an example is presented in Figure 9. The displacements and relative intensities of shake-up satellites can sometimes be useful in identifying the chemical state of an element, as discussed in Section I.5.C., p. 20.

vi. Multiplet Splitting. Emission of an electron from a core level of an atom that itself has a spin (unpaired electrons in valence levels)

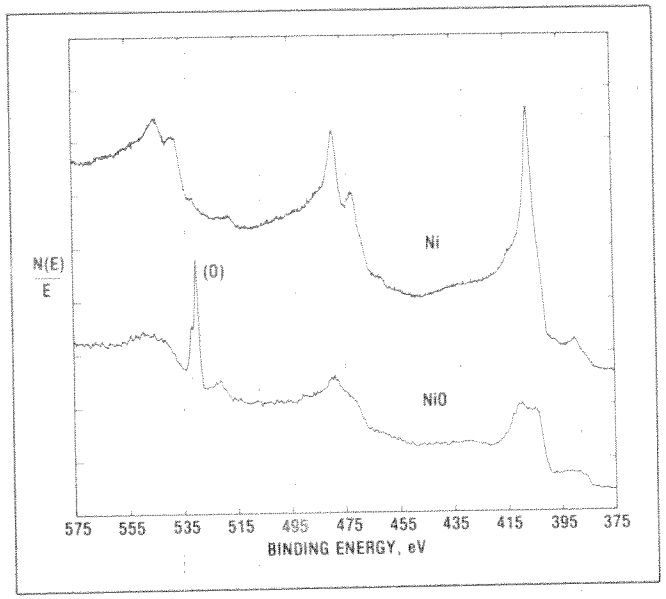

Figure 9. Some effects of chemical state on Auger line shapes.

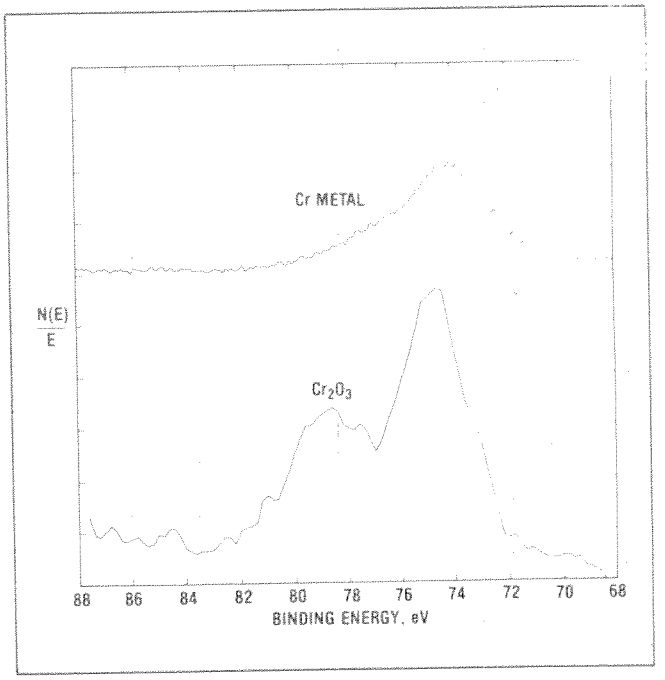

Figure 10. Multiplet splitting in the Cr 3s line.

can create a vacancy in two or more ways. The coupling of the new unpaired electron left after photoemission from an s-type orbital with other unpaired electrons in the atom can create an ion with either of two configurations and two energies. This results in a photoelectron line that is split asymmetrically into two components similar to the one shown in Figure 10.

Splitting also occurs in the ionization of p levels, but the result is more complex and subtle. In favorable cases, it results in an apparent slight increase in the spin doublet separation, evidenced in the separation of the $2p_{1/2}$ and $2p_{3/2}$ lines in first row transition metals, and the generation of a less easily noticed asymmetry in the line shape of the components. Often such effects on the p doublet are obscured by shake-up lines.

vii. Energy Loss Lines. With some materials, there is an enhanced probability for loss of a specific amount of energy due to interaction between the photoelectron and other electrons in the surface region of the sample. An example of this is shown in Figure 11. The enhanced probability of energy loss produced a distinct and rather sharp hump at an energy about 21 eV above the binding energy of the parent line. Under certain conditions of spectral display, energy loss lines can cause confusion. Such phenomena in insulators are rarely sharper than that shown in Figure 11, and are usually much more muted. They are, of course, different in each solid medium.

With metals, the effect is often much more dramatic, as indicated by the loss lines for

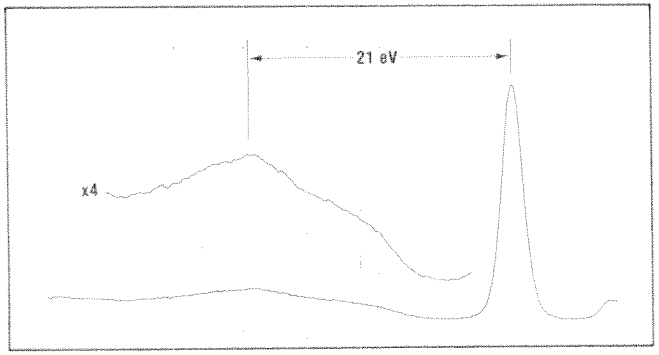

Figure 11. Energy loss envelope from the O1s line in SiO_2.

aluminum shown in Figure 12. Energy loss to the conduction electrons occurs in well-defined quanta characteristic of each metal. The photoelectron line, or the Auger line, is successively mirrored at intervals of higher binding energy, with reduced intensity. The energy interval between the primary peak and the loss peak is called the plasmon energy. The so-called "bulk plasmons" are the more prominent of these lines. A second series, the "surface plasmons", exists at energy intervals determined by dividing the bulk plasmon energy by $\sqrt{2}$. The effect is not easily observable in non-conductors, nor is it prominent in all conductors.

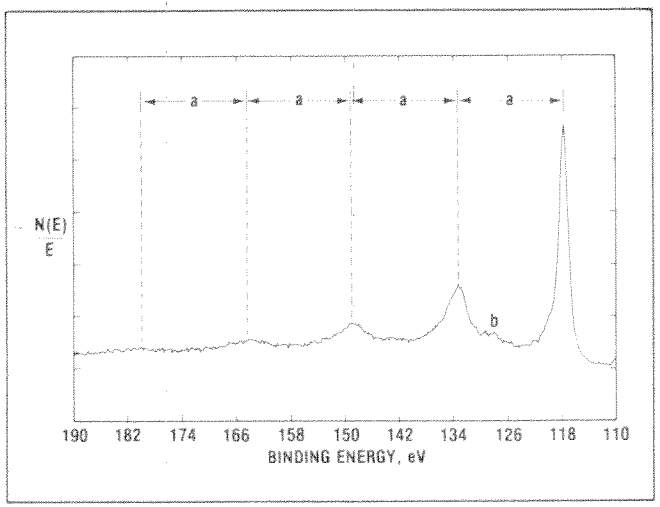

Figure 12. Energy loss (plasmon) lines associated with the 2s line of aluminum (a = 15.3eV; note surface plasmon at b).

viii. Valence Lines and Bands. Lines of low intensity occur in the low binding energy region of the spectrum between the Fermi level and about 10-15 eV binding energy. These lines are produced by photoelectron emission from molecular orbitals and from solid state energy bands. Differences between insulators and conductors are especially noted by the absence or presence of electrons from conduction bands at the Fermi level.

B. LINE IDENTIFICATION

In general, interpretation of the ESCA spectrum is most readily accomplished by first identifying the lines that are almost always present, specifically those of carbon and oxygen, then identifying major lines and associated weaker lines and, lastly, identifying the remaining weak lines. The following step-by-step procedure generally simplifies the data interpretation task and minimizes data ambiguities.

Step 1. The C1s, O1s, C(KLL) and O(KLL) lines are usually prominent in any spectrum. Identify these lines first along with all derived x-ray satellites and energy loss envelopes.

Step 2. Identify other intense lines (cf Appendix Tables) present in the spectrum. Then label any related satellites and other less intense spectral lines associated with those elements. Keep in mind that some lines may be interfered with by more intense, overlapping lines from other elements. The most

serious interferences by the carbon and oxygen lines, for example, are Ru3d by C1s, V2p and Sb3d by O1s, I(MNN) and Cr(LMM) by O(KLL), and Ru(MNN) by C(KLL).

Step 3. Identify any remaining minor lines. In doing this, assume they are the most intense lines of an unknown element. If not, they should already have been identified in previous steps. Again, possible line interferences should be kept in mind. Small lines that seem unidentifiable can be ghost lines. This possibility can be checked for the more intense parent photoelectron lines using Table 2 (p. 13).

Step 4. Check the conclusions by noting the spin doublets for p, d, and f lines. They should have the right separation (cf Appendix Tables 1 and 2, pp. 182 and 184) and should be in the correct intensity ratio. The ratio for p lines should be about 1:2, d lines 2:3, and f lines 3:4 except that p lines, especially 4p lines, may be less than 1:2.

C. CHEMICAL STATE IDENTIFICATION

The identification of chemical states depends primarily upon the accurate determination of line energies. To determine line energies accurately, the voltage scale of the instrument must be precisely calibrated (cf Section I.4.B., p. 10), a line with a narrow sweep range must be recorded with good statistics (of the order of several thousand counts per channel above background), and accurate correction must be made for static charge if the sample is an insulator.

(1) Determination of Static Charge on Insulators. During analysis, insulating samples tend to acquire a steady-state charge of as much as several volts. This steady-state charge is a balance between electron loss from the surface by emission and electron gain by conduction or by acquisition of slow or thermal electrons from the vacuum space. The steady-state charge, usually positive, can be minimized by adding slow electrons to the vacuum space with an adjacent neutralizer or flood gun. It is often advantageous to do this to reduce differential charging and to sharpen the spectral lines.

A serious problem is the exact determination of the extent of charging. Any positive charging adds to the retardation and tends to make the peaks appear at higher binding energy, whereas excessive compensation can make the peaks shift to lower binding energy. The following are five methods that are usually valid for charge correction on insulating samples:

i. Measurement of the position of the C1s line from adventitious hydrocarbon nearly always present on samples introduced from the laboratory environment or from a glove box. This line, on unsputtered inert metals such as gold or copper, appears at 284.6 eV, so any shift from this value can be taken as a measure of the static charge. (Much of the literature uses the more approximate value of 285). At this time, it is not known whether a reproducible line position exists for carbon remaining on the surface after ion beam etching.

ii. Evaporation of a trace of gold onto the sample after the spectra have been recorded. The Au4f doublet is then recorded as well as a repetition of the most important line in the sample spectrum. It is then assumed that the potential of the gold islands reflects the new steady-state charge of the surface of the sample. Care

must be taken to ensure that the gold is present in trace quantities so that the original spectrum is little affected. In this procedure there may well be a double correction. The steady-state potential after gold is deposited may well be different from the steady-state potential in the original sample before gold deposition.

iii. The use of an internal standard, such as a hydrocarbon moiety in the sample. The value of 284.6 eV for the C1s line is recommended.

iv. The use of an insulating sample so thin that it effectively does not insulate. This can be assumed if the spectrum of the underlying conductor appears in good intensity and line positions are not affected by changes in electron flux from the charge neutralizer.

v. For the study of supported catalysts or similar materials, one can adopt a suitable value for a constituent of the support and use that to interrelate binding energies of different samples. One must be certain that treatments of the various samples are not so different that the inherent binding energies of support constituents are changed.

Some precautions should be borne in mind. If the sample is heterogeneous on even a micrometer scale, particles of different materials can charge to different extents, and interpretation of the spectrum is complicated accordingly. One cannot physically mix a conducting standard like gold or graphite of micron dimensions with a powder and validly use the gold or graphite line in order to correct for static charge.

(2) Photoelectron Line Chemical Shifts and Separations. An important advantage of ESCA is the ability to obtain information on chemical states from the variations in binding energies, or chemical shifts, of the photoelectron lines. This has been extremely useful in many studies. While many attempts have been made to calculate chemical shifts and absolute binding energies, the factors involved, especially in the solid state, are imperfectly understood and one must rely on experimental data on standard materials. The tables accompanying the spectra in this Handbook record considerable data from the literature as well as data obtained specifically for this Handbook. All literature data have been carefully evaluated and corrected, and are believed reliable.[a] These data have been adjusted to the instrumental calibration and static charge reference values given above, and are, therefore, directly comparable.

Since occasional line interferences do occur, it is sometimes necessary to use a line other than the most intense one in the spectrum. Chemical shifts are very uniform among the photoelectron lines of an element, so that line separations rarely vary by more than 0.2 eV. However, exceptional separations can occur in paramagnetic materials because of multiplet splitting. Separations of photoelectron lines can be determined approximately from Tables 1 and 2 in the Appendix (pp. 182 and 184).

(3) Auger Line Chemical Shifts and the Auger Parameter. Core-type Auger lines (transitions

(a) In some cases, different binding energy values appearing in the literature for the same material could not be reconciled, and no grounds could be found for choosing one over the other. In such cases, more than one value is included to indicate the degree of uncertainty.

ending with double vacancies below the valence levels) usually have at least one component that is narrow and intense, often nearly as intense as the strongest photoelectron line (cf. spectra for F, Na, As, In, Te, and Pb). There are four core Auger groups that can be generated by Mg or Al x-rays: the KLL (Na, Mg); the LMM (Cu, Zn, Ga, Ge, As, and Se); the MNN (Ag, Cd, In, Sn, Sb, Te, I, Xe, Cs, and Ba); and the NOO (Au, Hg, Tl, Pb, and Bi). The MNN lines in the rare earths, while accessible, are very broad because of multiplet splitting and shake-up phenomena with most of the compounds. Valence-type Auger lines (final states with vacancies in valence levels), such as those for O and F (KLL); Mn, Fe, Co, and Ni (LMM); and Ru, Rh, and Pd (MNN), can be intense and are, therefore, also useful. Chemical shifts occur with Auger lines as well as with photoelectron lines. The chemical shifts are different from those of the photoelectron lines, however, and usually are considerably more pronounced. This can be very useful for identification of chemical states, especially in combination with photoelectron chemical shift data. If data for the various chemical states of an element are plotted, with the kinetic energy of the photoelectron line on the abscissa and that of the Auger line on the ordinate, a two-dimensional chemical state plot is obtained. Such plots accompany the spectra for F, Na, Cu, Zn, As, Ag, Cd, In, and Te.

With chemical states displayed in two dimensions, the method becomes more powerful as a tool for identifying the chemical components. In the format adopted for the Handbook, the kinetic energy of the Auger line is plotted against the binding energy of the photoelectron line, with the latter plotted in the -x direction (kinetic energy is still, implicitly, +x). the kinetic energy of the Auger electron, referred to the Fermi level, is easily calculated by subtracting from the photon energy the position of the Auger line on the binding energy scale.

With this arrangement, each diagonal line represents all values of equal sums of Auger kinetic energy and photoelectron binding energy. A quantity called the Auger parameter, α, is defined as,

$$\alpha = KE_A - KE_P = BE_P - BE_A \quad (2)$$

or, the difference in binding energy between the photoelectron and Auger lines. This difference can be accurately determined because static charge corrections cancel. Then, with all kinetic energies and binding energies referenced to the Fermi level,

$$KE_P = h\nu - BE_{/P} \quad (3)$$

$$KE_A + BE_P = h\nu + \alpha \quad (4)$$

or, the sum of the kinetic energy of the Auger line and the binding energy of the photoelectron line equals the Auger parameter plus the photon energy. A plot showing Auger kinetic energy versus photoelectron binding energy then becomes independent of the energy of the photon.

In general, polarizable materials, especially conductive materials, have a high Auger parameter, while insulating compounds fall lower on the grid. The points on the two-dimensional plot are drawn as rectangular boxes at 45°, reflecting the expected error of measurement in the two perpendicular directions. At present, sufficient data for the two-dimensional chemical state plots are available only for the nine elements listed above.

(4) Chemical Information From Satellite Lines and Peak Shapes.

i. Shake-up Lines. These satellite lines have intensities and separations from the parent photoelectron line that are unique to each chemical state (Figure 8). Some Auger lines also exhibit radical changes with chemical state that reflect these processes (Figure 9). With transition elements and rare earths the absence of shake-up satellites is usually characteristic of the elemental or diamagnetic states. Prominent shake-up patterns typically occur with paramagnetic states. Table 3 has been included as a guide to some expected paramagnetic states.

ii. Multiplet Splitting. On occasion, the multiplet splitting phenomenon can also be helpful in identifying chemical states. The 3s lines in the first series of transition metals, for example, exhibit separations characteristic of each paramagnetic

Table 3 — General guide to paramagnetic species

Multiplet splitting and shake-up lines are generally expected in the paramagnetic states below.

Atomic No.	Paramagnetic States	Diamagnetic States
22	Ti^{+2}, Ti^{+3}	Ti^{+4}
23	V^{+2}, V^{+3}, V^{+4}	V^{+5}
24	Cr^{+2}, Cr^{+3}, Cr^{+4}, Cr^{+5}	Cr^{+6}
25	Mn^{+2}, Mn^{+3}, Mn^{+4}, Mn^{+5}	Mn^{+7}
26	Fe^{+2}, Fe^{+3}	$K_4Fe(CN)_6$, $Fe(CO)_4Br_2$
27	Co^{+2}, Co^{+3}	CoB, $Co(NO_2)_3(NH_3)_3$, $K_3Co(CN)_6$, $Co(NH_3)_6Cl_3$
28	Ni^{+2}	$K_2Ni(CN)_4$, square planar complexes
29	Cu^{+2}	Cu^{+1}
42	Mo^{+4}, Mo^{+5}	Mo^{+6}, MoS_2, $K_4Mo(CN)_8$
44	Ru^{+3}, Ru^{+4}, Ru^{+5}	Ru^{+2}
47	Ag^{+2}	Ag^{+1}
58	Ce^{+3}	Ce^{+4}
59-70	Pr, Nd, Sm, Eu, Gd, Tb, Dy, Ho, Er, Tm, Yb compounds	
74	W^{+4}, W^{+5}	W^{+6}, WO_2, WCl_4, WC, $K_4W(CN)_8$
75	Re^{+2}, Re^{+3}, Re^{+4}, Re^{+5}, Re^{+6}	Re^{+7}, ReO_3
76	Os^{+3}, Os^{+4}, Os^{+5}	Os^{+2}, Os^{+6}, Os^{+8}
77	Ir^{+4}	Ir^{+3}
92	U^{+3}, U^{+4}	U^{+6}

chemical state. The 3s line, however, is weak and therefore is not often useful analytically. The 2p doublet separation is also affected by multiplet splitting and the lines are more intense. The effect becomes very evident with cobalt compounds where the separation varies up to one electron volt. Little utilization of this effect has yet been made. However, when first row transition metal compounds are under study, it may prove useful to record accurately these line separations and make comparisons with model compounds.

iii. Auger Line Shape. Valence type Auger transitions form final-state ions with vacancies in molecular orbitals. The distribution of the group of lines is strongly affected, therefore, by the nature of the molecular orbitals in the different chemical states. Although little has yet been published on this subject, the spectroscopist should bear in mind the possible utility of Auger line shapes of oxygen, fluorine, the first row transition metals (Sc-Ni), and Ru, Rh, and Pd.

D. QUANTITATIVE ANALYSIS

For many ESCA investigations, it is important to determine the relative concentrations of the various constituents. Methods for quantifying the ESCA measurement utilizing peak area sensitivity factors and peak height sensitivity factors have been developed. The method which utilizes peak area sensitivity factors typically is the more accurate and is discussed below. The method for determining peak height and peak area is shown in Figure 13. This approach is satisfactory for quantitative work except with transition metal spectra with prominent shake-up lines. For these, it is often better to include the entire 2p region when measuring peak area.

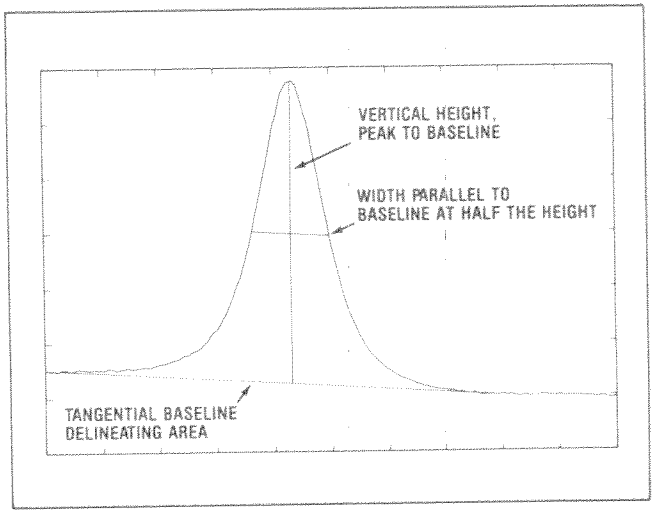

Figure 13. Method for determining height, width, and area of a photoelectron peak.

For a sample that is homogeneous in the analysis volume, the number of photoelectrons per second in a specific spectral peak is given by:

$$I = nf\sigma\theta y\lambda AT \qquad (5)$$

where n is the number of atoms of the element per cm^3 of sample, f is the x-ray flux in photons/cm^2-sec, σ is the photoelectric cross-section for the atomic orbital of interest in cm^2, θ is an angular efficiency factor for the instrumental arrangement based on the angle between the photon path and detected electron, y is the efficiency in the photoelectric process for formation of photoelectrons of the normal photoelectron energy, λ is the mean free path of the photoelectrons in the sample, A is the area of the sample from which photoelectrons are detected, and T is the detection efficiency for electrons emitted from the sample. From (5):

$$n = I/f\sigma\theta y\lambda AT \qquad (6)$$

The denominator in equation 6 can be assigned the symbol S, defined as the atomic sensitivity factor. If we consider a strong line from each of two elements, then:

$$\frac{n_1}{n_2} = \frac{I_1/S_1}{I_2/S_2} \qquad (7)$$

This expression may be used for all homogeneous samples if the ratio S_1/S_2 is matrix independent for all materials. It is certainly true that such quantities as σ and λ vary somewhat from material to material (especially λ), but the ratio of each of the two quantities σ_1/σ_2 and λ_1/λ_2, remains nearly constant. Thus, for any spectrometer, we may develop a set of relative values of S for all of the elements.

A generalized expression for determination of the atom fraction of any constituent in a sample, C_x, can be written as an extension of equation 7:

$$C_x = \frac{n_x}{\sum_i n_i} = \frac{I_x/S_x}{\sum_i I_i/S_i} \qquad (8)$$

Values of S based on peak area measurements are indicated in Table 5 of the Appendix. These values are presented relative to the F1s intensity, which has been used as a standard. The values of S in the Appendix are based upon calculated values of σ[a] which have been corrected for the kinetic energy dependence of the spectrometer detection efficiency and an average value for the dependence of λ on kinetic energy of $E^{0.75}$ (Figure 3). The values in the Appendix are only valid for, and should only be applied, when the electron energy analyzer used has the transmission characteristics of the double pass cylindrical-mirror type analyzer supplied by Physical Electronics. An example of the application of equation 8 to analysis of a nearly ideal sample, polytetrafluoroethylene, is shown in Figure 14.

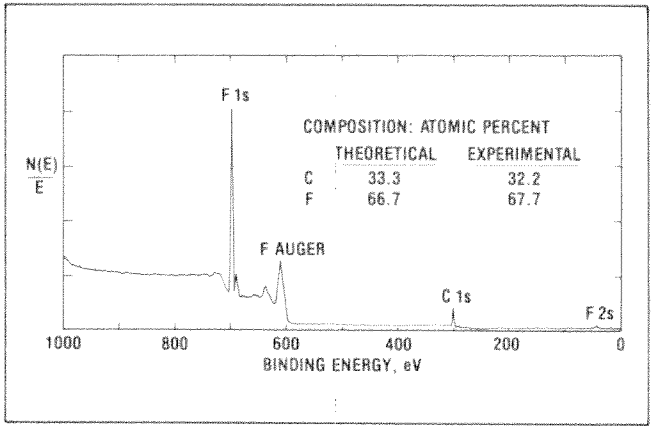

Figure 14. Quantitative analysis of polytetrafluoroethylene (by peak area of F1s and C1s).

The use of atomic sensitivity factors in the manner described will normally furnish semiquantitative results (within 10-20%) except in the following situations.

(1) The technique cannot be applied rigorously to heterogeneous samples. It can be useful with heterogeneous samples in obtaining results in terms of the relative number of atoms detected, but one must be conscious that the microscopic character of the heterogeneous system influences the quantitative results. Moreover, an overlying contamination layer has the effect of diminishing high binding energy peaks more than those with low binding energies.

(2) Transition metals, especially of the first series, have widely varying and low values of y, whereas y for the other elements is rather

a) J. H. Scofield, J. Elect. Spectr. 8, 129 (1976).

uniform at about 0.8. Thus, a value of S determined on one chemical state for a transition metal may not be valid for another chemical state.

(3) When peak interferences occur, alternative lines must sometimes be used. The ratios of spin doublets (except 4p) are rather uniform and the weaker of the pair can often be substituted. Figure 15 is a general guide to the relative peak height of the minor lines. However, with the minor lines, there is much variation in relative peak heights and widths, so the figure should be regarded as a semi-quantitative guide, of the order of ±30%. The sample spectra of the elements may also be consulted, but caution must be exercised, since the spectra of the elements themselves can be somewhat different, quantitatively, from the spectra of their compounds.

Occasionally an x-ray satellite from an intense photoelectron line interferes with measurement of a weak component. A mathematical approach can then be used to subtract the x-ray satellite before the measurement.

For quantitative work it is advisable to check the spectrometer operation frequently to ensure that analyzer response is constant and optimum. A useful test is the recording of the three widely-spaced spectral lines from copper. Measurement of peak height in counts per second should be made on 20 volt wide scans of the $2p_{3/2}$, LMM Auger, and 3p lines, and the peak width of the $2p_{3/2}$ line should be measured as shown in Figure 13. Maintenance of such records makes it easily noticeable if an instrumental change occurs that would affect quantitative analysis.

E. DETERMINATION OF ELEMENT LOCATION

(1) Depth. There are four methods of obtaining information on the depth of an element in the sample. The first two methods below utilize the characteristics of the spectrum itself, but provide limited information. The third, depth profiling by erosion of the surface, provides more detailed information but is attended by certain problems. The fourth utilizes measurements at two or more electron escape angles.

i. The presence or absence of an energy loss peak or envelope indicates whether the emitting atoms are in the bulk or at the surface. Since electrons from surface atoms do not traverse the bulk, peaks due to the surface atoms are symmetrical above level baselines on both sides and the energy loss peak is absent.

ii. Elements whose spectra exhibit photoelectron lines widely spaced in kinetic energy can be approximately located by noting the intensity ratio of the lines. In the energy range above approximately 100 eV, electrons moving through a solid with lower kinetic energy are attenuated more strongly than those with higher kinetic energy. Thus, for a surface species, the low kinetic energy component will be relatively stronger than the high kinetic energy component, compared to that observed in the pure material. The data in Figure 15 for homogeneous bulk solids can be compared with intensity ratios observed on unknowns to determine qualitatively the distribution of the element in the sample. Suitable elements include Na and Mg (1s and 2s); Zn, Ga, Ge, and As ($2p_{3/2}$ and 3d); and Cd, In, Sn, Sb, Te, I, Cs, and Ba ($3p_{3/2}$ and 4d, or $3d_{5/2}$ and 4d).

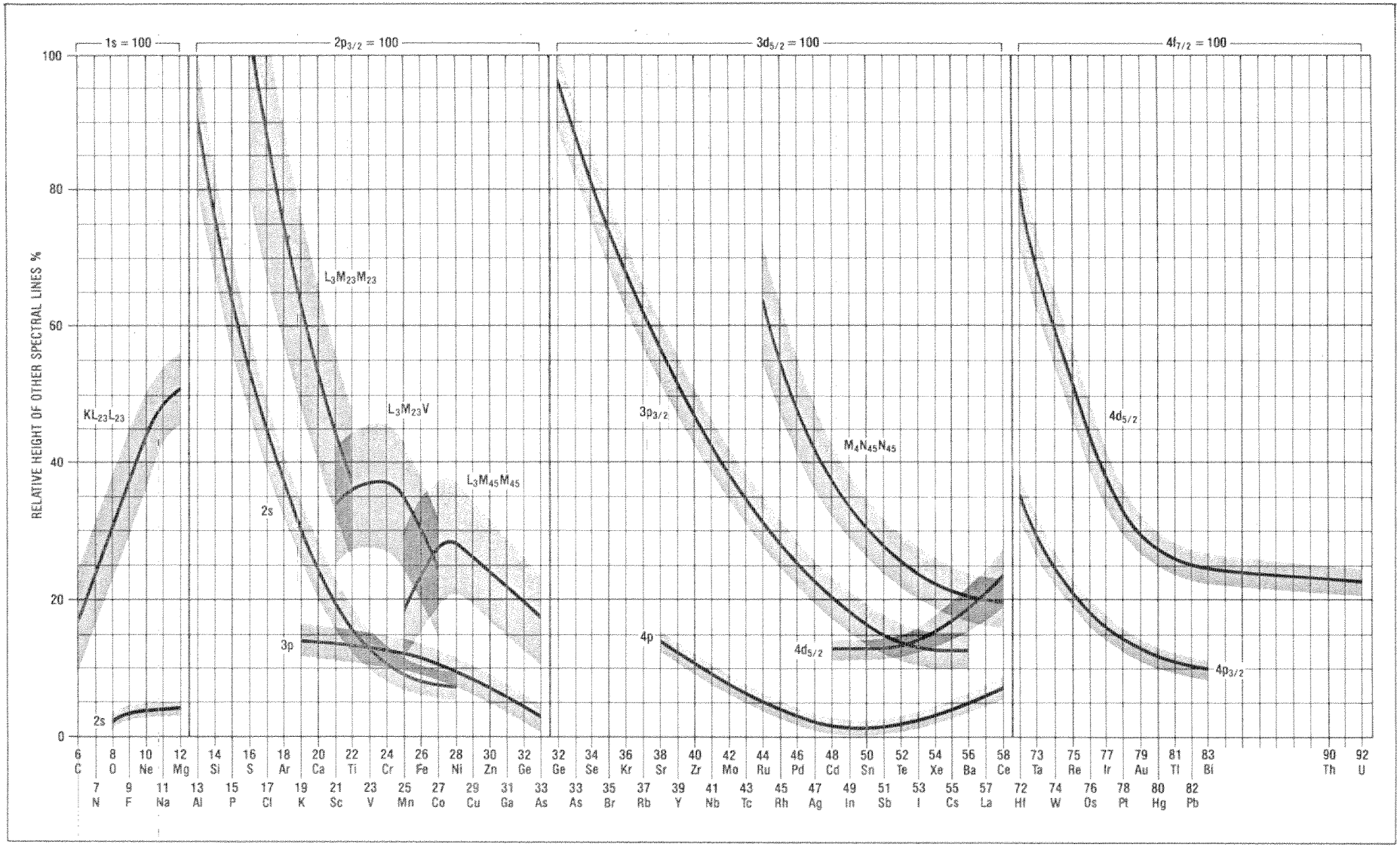

Figure 15. Peak heights of minor lines relative to strong lines (based on survey spectra contained herein).

For the situation where the element is in a bulk homogeneous layer beneath a thin contaminating layer the characteristic intensity ratio is modified in the opposite direction. Thus, for a pair of lines due to subsurface species, the low kinetic energy line will be attenuated more than the high kinetic energy line, distorting the characteristic intensity ratio. By observing such intensity ratios and comparing them with the values for pure bulk elements (Figure 15), it is possible to deduce whether the observed lines are due to predominantly surface, subsurface, or homogeneously distributed material.

iii. Depth profiling can be accomplished by controlled erosion of the surface by ion sputtering. In Table 4 are presented some data on sputter rates as a general guide. One can use this technique on organic materials, but few data are available for calibration. Chemical states are usually changed by the sputter technique, but useful information on elemental distribution still can be obtained.

Table 4 — Some representative sputter rates

(2 keV argon ion beam with 100 μamps/cm² impinging on sample)

Target	Sputter Rate, Å/min[a)]
Ta_2O_5	100
Si	90
SiO_2	85
Pt	220
Cr	140
Al	95
Au	410

a) ± 20%.

Another method of controlled erosion tha is useful, especially with organic materials is reaction with oxygen atoms from a plasma. This technique may also change the chemical states in the affected surface Further, since the elements differ in their rates of reaction with oxygen atoms, the rate of removal of surface materials will be somewhat sample dependent.

iv. One may alter the angle between the plane of the sample surface and the angle of entrance to the analyzer. At 90°, with respect to the surface plane, the signal from the bulk is maximized relative to that from the surface layer. At small angles, the signal from the surface becomes greatly enhanced, relative to that from the bulk. The location of an element can thus be deduced by noting how the magnitude of its spectral peaks change with sample orientation in relation to those from other elements.

The electron energy analyzer used in the ESCA/SAM incorporates a special aperture arrangement that permits angular resolved studies. An example of the information that can be gained through the use of this capability is shown in Figure 16. Data were obtained at high (near 90°) and low (near 15°) exit angles from a silicon sample with a thin silicon oxide overlayer. The observed intensity ratio of oxidized to elemental silicon is much greater at the small exit angle.

(2) Insulating Domains on a Conductor. The occurrence of steady-state charging of an insulator during analysis sometimes has useful consequences. Microscopic insulating domains on a conductor reach their own steady-

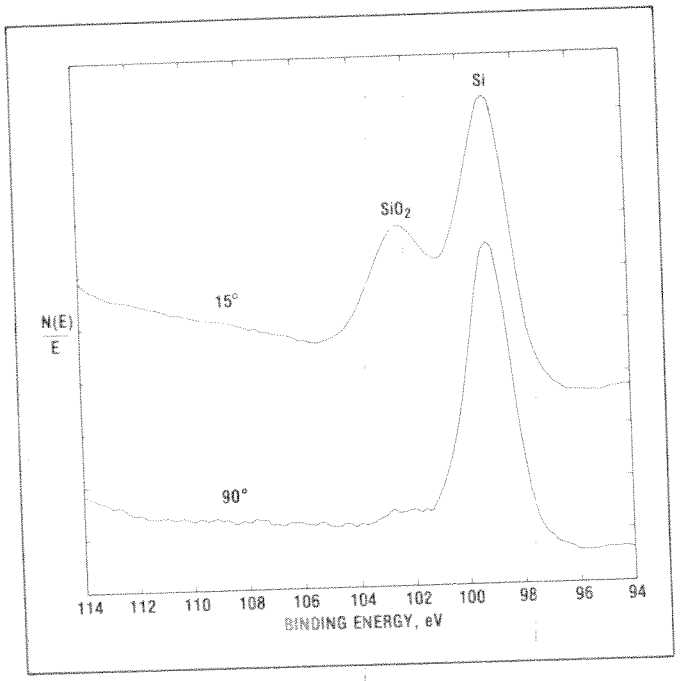

Figure 16. Use of different electron escape angles to determine depth distribution (Si 2p line from silicon sample with approximately one monolayer SiO_2 overlayer). Angles indicated are electron take-off angles relative to specimen surface.

state charge, while the conductor remains at spectrometer potential. Thus, an element in the same chemical state in both phases will exhibit two peaks. If a change is made in the supply of low energy electrons which stabilize the charge, as from the neutralizer filament, or if a bias is applied to the conductor, the spectral peaks from the insulating phase will move relative to those from the conducting phase, as shown in Figure 17. For such heterogeneous systems, this is an extremely useful technique. It makes it possible to determine whether the elements that contribute to the overall spectrum are in the conducting or the insulating phase, or in both phases.

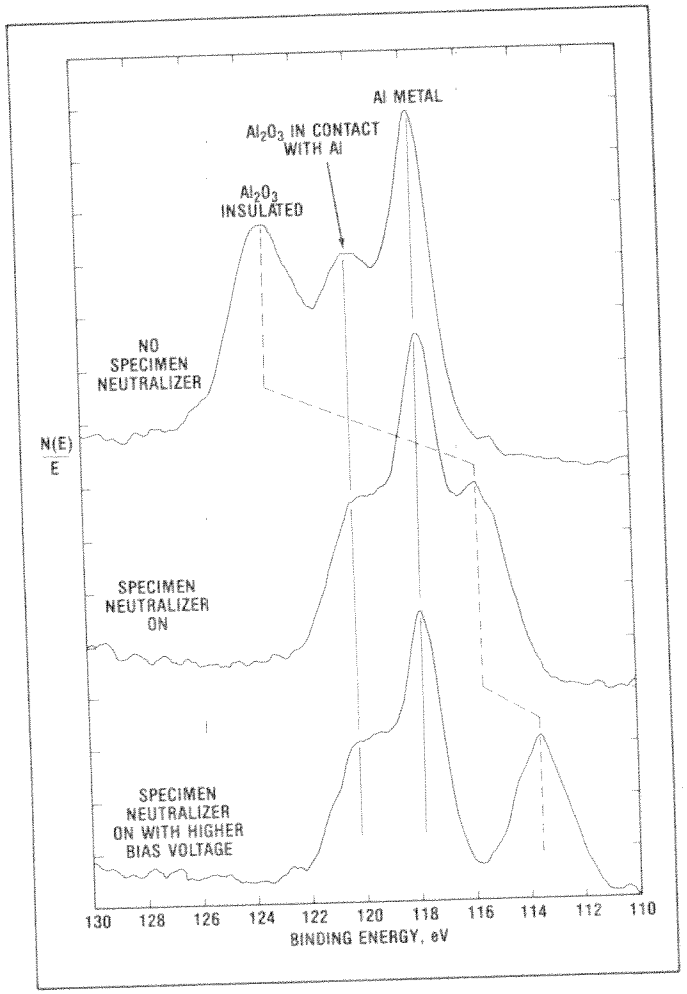

Figure 17. Use of specimen neutralizer to shift the partial spectrum from insulating domains (Al 2s lines from Al_2O_3 on aluminum sample).

(3) Surface Distribution. ESCA is not ordinarily used to obtain information on X-Y distribution because a large analysis area is required for good signal intensity. With the PHI double pass cylindrical-mirror analyzer used in the ESCA/SAM, however, a circular area of 2-5 mm diameter can be imaged, depending upon the apertures in use and the retarding condi-

tions. This area is expressed as the full width at half maximum of the photoelectron intensity observed as a function of distance from the center of the imaged area. Thus, the effective sample area is not large. It is often possible to analyze different positions on the same sample when the surface is heterogeneous on a scale larger than two millimeters.

6. How to Use This Handbook

Full utilization of this Handbook can best be accomplished by following these procedures.

A. FOR QUALITATIVE ANALYSIS

The elemental and chemical identification of sample constituents can be performed most readily by combining the information in the standard survey spectra in Section II with the binding energy tables (Tables 1-4) presented in the Appendix.

(1) First identify all major photoelectron peaks utilizing the line position tables (Tables 1-4, pages 182-187).

(2) Check to see that the determinations made in step 1 are consistent with the standard survey spectra.

(3) Identify the Auger electron peaks by the line positions listed in Tables 1-4 in the Appendix (these are different for Mg and Al x-ray sources) and the expanded spectra provided for many of the elements in Section II.

(4) Review section I.5.A. (p. 12) to account for fine structure such as energy loss lines, shake-up peaks, satellite lines, etc. not identified in Handbook spectra or energy tables.

(5) Identify any remaining small peaks, assuming they are intense photoelectron or Auger lines of minor constituents using Tables 3 and 4.

(6) Chemical state identification can be deduced from high energy resolution ($E_{pass} \leq 25$ eV) spectra of the strongest photoelectron lines and sharpest Auger lines.

i. Review Section I.5.C. (p. 17) to correct binding energies for static charging of insulators. When applicable, charge reference the binding energy scale to the hydrocarbon C1s photoelectron peak (BE = 284.6 eV).

ii. Use the tabulated experimental data and standard high energy resolution spectra to determine the chemical state from measured shifts in the photoelectron binding energies (cf section I.5.C., p. 18).

iii. For the elements F, Na, Cu, Zn, As, Cd, In, and Te, convert corrected Auger line positions to kinetic energies by subtracting from the photon energy (Mg = 1253.6, Al = 1486.6 eV). Note the location of the points for Auger kinetic energy and photoelectron binding energy on the respective elemental plot. Proximity of experimental points to